*minerals*

MDPI

*Article*

# Hydrogen Peroxide Ammonium Citrate Extraction: Mineral Decomposition and Preliminary Waste Rock Characterization

**Teemu Karlsson [1,2,*], Marja Liisa Räisänen [3,†], Timo Myöhänen [4], Lena Alakangas [2], Marja Lehtonen [5] and Päivi Kauppila [1]**

1 Circular Economy Solutions, Geological Survey of Finland, 70211 Kuopio, Finland; paivi.kauppila@gtk.fi
2 Department of Civil, Environmental and Natural Resources, Division of Geosciences and Environmental Engineering, Luleå University of Technology, 97187 Luleå, Sweden; lena.alakangas@ltu.se
3 Industrial Environments and Recycling, Geological Survey of Finland, 70211 Kuopio, Finland; marja.raisanen@pp1.inet.fi
4 Eurofins Labtium Oy, 70211 Kuopio, Finland; timo.myohanen@iki.fi
5 Circular Economy Solutions, Geological Survey of Finland, 02151 Espoo, Finland; marja.lehtonen@gtk.fi
* Correspondence: teemu.karlsson@gtk.fi; Tel.: +358-50-565-1370
† Retired.

**Abstract:** A commonly-used method in ore exploration is hydrogen peroxide ammonium citrate (HA) extraction, which has not typically been used in waste rock characterization. In this study, the sulfide specificity and leaching of other minerals in HA extraction was evaluated and its performance was compared with the aqua regia (AR) extraction for preliminary assessment of harmful element mobility. Samples collected from several different mine sites in Finland were utilized. The waste rock sample S contents ranged from 0.3% to 5.3%, and sums of the AR extractable elements As, Cd, Co, Cu, Ni and Zn range from 120 to 8040 mg/kg. The drainage types ranged from acid high-metal to neutral low-metal, with pH's of 3.3–7.7. Mineralogical changes that took place in the HA solution were investigated by the field emission scanning electron microscope (FE-SEM) equipped with an energy-dispersive X-ray spectroscopy analyzer (EDS) and X-ray diffraction (XRD) methods. Results of the study showed that the HA extraction appears to be a more specific method for sulfide decomposition compared with AR extraction. Sulfide minerals, especially base metal sulfides pentlandite, chalcopyrite and sphalerite, decomposed efficiently in HA extraction. However, the Fe-sulfides pyrrhotite and pyrite only decomposed incompletely. The study showed that the HA extraction results can be used in the preliminary prediction of element mobility. Based on the results, the elevated As, Cd, Co, Cu, Ni, S and Zn leachability in the HA extraction appears to predict elevated drainage concentrations. If the HA-extractable sum of As, Cd, Co, Cu, Ni and Zn is >750 mg/kg, there is an increased risk of high-metal (>1000 µg/L) drainage. Therefore, the HA extraction data, e.g., produced during ore exploration, can be utilized to preliminary screen the risks of sulfide related element mobilities from waste rock material.

**Keywords:** mine waste characterization; ARD; NRD; aqua regia extraction; sulfide decomposition; SEM mineralogy

check for updates

**Citation:** Karlsson, T.; Räisänen, M.L.; Myöhänen, T.; Alakangas, L.; Lehtonen, M.; Kauppila, P. Hydrogen Peroxide Ammonium Citrate Extraction: Mineral Decomposition and Preliminary Waste Rock Characterization. *Minerals* **2021**, *11*, 706. https://doi.org/10.3390/min11070706

Academic Editors: Benoît Plante, Thomas Pabst and David Wilson

Received: 17 May 2021
Accepted: 28 June 2021
Published: 30 June 2021

**Publisher's Note:** MDPI stays neutral with regard to jurisdictional claims in published maps and institutional affiliations.

**Copyright:** © 2021 by the authors. Licensee MDPI, Basel, Switzerland. This article is an open access article distributed under the terms and conditions of the Creative Commons Attribution (CC BY) license (https://creativecommons.org/licenses/by/4.0/).

## 1. Introduction

Sulfides are essential for the mining industry as important metal ore minerals [1]. However, sulfides are also the main source of contaminated rock drainage, acid (ARD) or neutral (NRD), which are considered to be the main environmental concerns related to mine waste management [2–6]. Sulfide minerals are prone to oxidization under the influence of atmospheric oxygen and water, a process that creates sulfuric acid, affects the pore water pH and Eh conditions and enhances the decomposition of other minerals [6,7].

For ore exploration purposes, a sulfide specific element extraction method is of importance because, besides being bound to sulfides, valuable elements may also be abundant

in the less economic silicate plus oxide fraction of a sample [8,9]. Selective extractions are also used to study the mobility of harmful elements from mine waste materials [10]. As sulfides are the primary sources of contaminants in mine wastes, a sulfide-specific extraction method is useful in environmental studies to assess the mobility of harmful elements [11]. It is important to characterize mine wastes and assess their behavior early in a mining project, as designing appropriate waste facilities and drainage water management systems is essential for mitigating the potential consequences of harmful drainage. Short-term laboratory analyses, including geochemical extraction methods, are usually good for preliminary investigation and screening, and the results can be used to select suitable samples for more thorough kinetic testing, e.g., humidity cell testing [12].

Aqua regia (AR) extraction, a 3:1 mixture of hydrochloric acid and nitric acid [11,13], is the most used extraction method in mineral exploration and mining environmental studies in Finland. For example, AR extraction is the preferred method for evaluating whether mine waste is inert [14]. AR dissolves elements bound especially to the sulfide fraction, but it also decomposes all carbonates and secondary minerals, and partly some silicates [11,13]. In general, the AR-extractable concentrations of waste rocks indicate well which contaminants are most likely to be of concern in waste rock drainage [15–19]. For some circumneutral drainage systems, the AR extraction might be too aggressive for drainage quality prediction [18]. Furthermore, as some minerals that are not likely to be soluble in natural waste rock systems are relatively soluble in AR, the method can overestimate the mobility of elements primarily bound to silicates and oxides, e.g., Al and Cr [18].

Other sulfide specific extraction methods, used mainly in ore exploration, include the hydrogen peroxide ammonium citrate (HA) extraction [20], brominated water extraction [21], bromine-methanol extraction [22], brominated water-carbon tetrachloride [23] and hydrogen peroxide-ascorbic acid extraction [9]. Although HA has been noted not to leach sulfides completely [22,24], it is a straightforward and relatively efficient method, and therefore commonly used especially in Ni and Co exploration [25–27]. According to Karlsson et al. [18], a $H_2O_2$-based extraction method might be more selective for element mobility assessment in circumneutral drainage systems compared with the more aggressive AR extraction. It would be beneficial, if the same methods that provide data for exploration, could be utilized in the environmental characterization of potential waste rocks already early in the mining project.

The objectives of this study were to: (1) evaluate the sulfide specificity, leaching of other minerals and the release of harmful elements in the HA extraction and (2) investigate the functionality of the HA extraction for the preliminary assessment of harmful element mobility from the waste rock material. To achieve these objectives, we compared the HA extraction with the more investigated AR extraction, utilizing waste rock samples collected from various Finnish mine waste sites representing different deposit types. Modern mineralogical analysis methods were used to determine mineralogical changes in the HA extraction. Furthermore, we compared the HA extraction results with the existing AR and drainage data presented by Karlsson et al. [18].

## 2. Materials and Methods

For a detailed study of the HA and AR extractions, six waste rock samples (WR1-5b) consisting of one piece of rock were collected from five different mine sites (Table 1). From Mine 5, two separate samples were taken from the same waste rock type (WR5a and WR5b). The samples from Mine 5 were collected directly from the production, thus being fresh, un-weathered samples. The other samples were also relatively un-oxidized looking pieces of rocks collected from the waste rock pile surfaces. Furthermore, HA extractions were also applied to 10 powdered composite waste rock samples from Mines A to Mine H. These samples were collected in a previous study by Karlsson et al. [18], where the performance of the single-addition net acid generation (NAG) test leachate analysis and the AR extraction in drainage quality prediction was studied. These composite waste rock samples consisted of ≈15–20 kg of heterogeneous pieces of rocks with diameters of

≈5–10 cm collected randomly from the surface of waste rock piles. The results for the AR extraction from Karlsson et al. [18] were used in this study to evaluate the efficiency of the HA extractions.

**Table 1.** The target mine sites and investigated waste rock samples WR1-5b for a detailed study of the HA and AR extractions.

| Mine | Sample | Deposit Description | Sulfides Related to the Deposit | Waste Rock Pile Active | Reference |
|---|---|---|---|---|---|
| Mine 1 (Talc, Ni) | WR1 | Palaeoproterozoic (1.9 Ga), mixed hydrothermal deposit, closely associated with a lens of massive serpentinite, consisting of magnesite pods, lenses within talc-magnesite rock and talc- rich schistose soapstone. | Pentlandite, pyrrhotite, chalcopyrite, pyrite | 2004– | [28] |
| Mine 2 (Cu, Co, Zn, Ni, Au) | WR2 | Palaeoproterozoic (1.9 Ga) mafic-ultramafic mixed hydrothermal VMS, disseminated sulfide ore hosted by quartz rock and metacarbonate rock. | Pyrite, pyrrhotite, chalcopyrite, sphalerite | 2012– | [29] |
| Mine 3 (Ni, Co) | WR3 | Palaeoproterozoic (1.9 Ga) magmatic ultramafic intrusion-hosted nickel deposit, consisting of closely spaced serpentinite massifs surrounded by migmatised mica gneiss. | Pyrrhotite, pentlandite, chalcopyrite, vallerite, mackinawite, cubanite | 1970–1993 | [30,31] |
| Mine 4 (Cu) | WR4 | Palaeoproterozoic (1.9 Ga) mafic basinal hydrothermal SedEx (sedimentary exhalative) deposit, ore appearing as brecciated and disseminated in amphibole host rock. | Chalcopyrite, cubanite, pyrrhotite, with lesser amounts of pyrite, sphalerite, pentlandite, mackinawite, molybdenite, bornite, and other Fe- and Cu-containing sulfides. | 1966–1984 | [32–35] |
| Mine 5 (Ni, Cu, PGE) | WR5a, WR5b | Palaeoproterozoic (2.1 Ga) mafic-ultramafic magmatic deposit hosted within a composite ultramafic layered intrusion, ore appearing in olivine pyroxenite as disseminated sulfides. | Pyrrhotite, pentandite and chalcopyrite | 2012– | [36] |

The rock samples were treated and analyzed in a laboratory of Labtium Oy/Eurofins Labtium Oy, which has been accredited by FINAS (Finnish Accreditation Service, Helsinki, Finland) in accordance with the ISO/IEC 17025 standard [37]. The samples were first dried at <40 °C and then crushed (>70% <2 mm). For the laboratory analyses, the crushed samples were split using a riffle splitter and/or the cone and quartering method, and representative sub-samples were milled in a steel container. The total concentrations of S were determined according to the ISO 15178 [38] standard, using a pyrolytic method (Eltra) and infrared (IR) detection. Main and trace element concentrations were determined with a hot AR extraction method and ICP-OES/MS techniques [11], using a modified version of the ISO-11466 standard [39] to dissolve the samples.

The HA extraction method was conducted as a modified version of the method described by Young [40]. The reagents included a solution made of 151 g of di-ammonium

hydrogen citrate $C_6H_8O_7 \bullet 2\ NH_3$ dissolved in 2000 mL of $H_2O$, and hydrogen peroxide (30% m/V). To the solid samples of 0.30 g, 15 mL of ammonium citrate solution and 7.5 mL hydrogen peroxide were added. The samples were shaken in 200 rpm for 2 h, after which they were centrifuged in 2300 rpm for 20 min. The solutions were diluted and analyzed by ICP-OES/MS techniques.

HA extraction was carried out as a parallel (HA1) and sequential (HA2) extraction with AR extraction (AR1 and AR2, respectively). In the latter, the AR2 extraction was carried out on the residue of the HA2 extraction. The AR2 results were adjusted for the original sample mass by a correlation factor (mass of residue/mass of original sample). The HA2 was conducted on a larger scale, to provide sufficient amounts of extraction residue for the mineralogical studies and sequential AR2 extractions. For this larger scale (150-fold) test, the amount of sample material was 45 g, with the amounts of reagents adjusted accordingly. Parallel extractions were made for all waste rock samples, and sequential extractions for the samples WR1-5b.

The quality of the geochemical waste rock analysis was assured by the accredited laboratory by analyzing control samples and providing the quality control analysis results along with the sample results. In addition, three parallel analyses were performed for HA1. For geochemical data analysis, detector readings below the detection limit (DL) were replaced by a value of 0.5 DL.

The mineralogical composition of the samples WR1-5b was studied before and after the HA2 extractions from the powdered materials for geochemical analyses, and HA2 residue materials, respectively. Mineralogical analyses were conducted at the GTK Research Laboratory by field emission scanning electron microscope (FE-SEM): JEOL (Tokyo, Japan) JSM7100F Schottky combined with an Oxford Instruments (Abingdon, UK) energy-dispersive X-ray spectroscopy (EDS) spectrometer X-Max 80 $mm^2$ (SDD). The powdered sample materials for the geochemical analyses, and the HA2 residue materials were used to prepare mineralogical polished samples cast in epoxy and covered with graphite to enhance electric conductivity. To investigate the modal mineralogy, around 10,000 individual mineral particles were analyzed from each sample utilizing INCA Feature software by Oxford Instruments. The mineralogical composition results obtained by the FE-SEM-EDS method are semi-quantitative and were normalized to 100%.

Minerals were identified by comparing the element composition obtained from the EDS spectra with the mineralogical database of GTK. Specific identification of minerals is not always possible, as e.g., carbon and OH and $H_2O$ groups are not shown in the EDS spectra. This should be considered when examining the mineralogical results. To ensure the quality of the FE-SEM-EDS analyses, the identification of the main mineral phases was verified by X-ray diffraction (XRD) method utilizing Bruker (Mannheim, Germany) D8 DiscoverA25 equipment. Further quality assurance measures included the routinely monitoring of the mineral classifications based on the GTK mineral database, and the manual checking of the analytical data that were left unclassified.

## 3. Results

### *3.1. Mineralogical Results*

Table 2 presents the mineralogical analysis results of the samples WR1-WR5b before the HA2 extraction, and the mineralogy after the HA2 extraction. The detailed mineralogical analysis results are presented in Table S1. Backscattered electron images of before and after the HA2 extraction are presented in Figures S1–S6.

**Table 2.** Mineralogy of the samples before and after the HA2 extraction based on FE-SEM-EDS. Values presented as grams, mineral masses calculated with the wt. % and the total mass of the sample (g).

| Mineral | WR1 | | WR2 | | WR3 | | WR4 | | WR5a | | WR5b | |
|---|---|---|---|---|---|---|---|---|---|---|---|---|
| | Before | After | Before | After | Before | After | Before | After | Before | After | Before | After |
| | | | | | Silicates | | | | | | | |
| Quartz | 20.94 | 12.17 | 8.39 | 13.16 | 11.39 | 7.89 | 2.40 | 1.69 | 0.06 | 0.14 | | |
| Biotite | 4.97 | 5.56 | 7.58 | 12.31 | 9.53 | 15.86 | 0.55 | 0.66 | 0.75 | 0.85 | | |
| Plagioclase (other than albite) | 3.01 | 2.04 | 12.31 | 5.86 | 4.35 | 3.97 | 20.72 | 16.56 | | | | |
| Albite | 0.67 | 0.60 | 1.96 | 0.80 | 2.18 | 1.03 | 0.79 | 0.44 | | | | |
| Diopside | | | | | | | | | 14.60 | 19.30 | 12.82 | 16.25 |
| Tremolite | 2.85 | 2.96 | 2.52 | 1.24 | | | | | 4.71 | 5.18 | 5.19 | 6.39 |
| Talc | 2.33 | 2.06 | | | | | | | | | | |
| K-feldspar | 0.68 | 0.24 | | | 0.69 | 0.38 | | | | | | |
| Chlorite | 0.40 | 0.86 | 0.36 | 0.60 | 0.48 | 0.68 | | | 0.98 | 1.13 | 0.43 | 0.46 |
| Phlogopite | 0.23 | 0.83 | 3.69 | 5.28 | 0.58 | 0.43 | | | | | | |
| Muscovite | 0.16 | 0.39 | 2.07 | 1.66 | 9.55 | 6.25 | | | | | | |
| Hornblende | | | 0.09 | 0.73 | 0.41 | 0.90 | 10.70 | 15.54 | 4.76 | 3.43 | 2.25 | 2.38 |
| Olivine | | | | | | | | | 1.47 | 1.53 | 1.56 | 1.44 |
| Augite | | | | | | | 5.16 | 3.88 | | | | |
| Actinolite | | | | | | | 1.62 | 2.04 | 5.50 | 2.52 | 7.35 | 4.32 |
| Epidote | | | | | | | 1.33 | 1.27 | | | | |
| Anthophyllite | | | | | | | | | 2.17 | 2.21 | 1.63 | 2.42 |
| Serpentine | | | | | | | | | 8.03 | 4.72 | 10.63 | 5.81 |
| Cordierite | | | | | 0.51 | 0.43 | | | | | | |
| Cummingtonite/Enstatite | | | | | | | | | 0.47 | 0.48 | 0.74 | 0.70 |
| Kaolinite | | | | | 1.22 | 1.03 | | | | | | |
| | | | | | Carbonates | | | | | | | |
| Magnesite | 4.61 | 1.68 | | | | | | | | | | |
| Dolomite | 1.33 | 0.14 | | | | | | | | | | |
| Calcite | | | 0.96 | 0.02 | | | 0.03 | 0.03 | | | | |
| | | | | | Sulfides | | | | | | | |
| Pyrrhotite | 1.66 | 0.31 | 0.31 | 0.22 | 3.15 | 1.15 | 0.05 | 0.00 | 0.26 | 0.20 | 0.32 | 0.41 |
| Pyrite | 0.29 | 0.05 | 4.50 | 0.08 | 0.07 | 0.00 | | | | | | |
| Pentlandite | 0.27 | 0.00 | | | 0.13 | 0.00 | | | 0.07 | 0.00 | 0.04 | 0.00 |
| Chalcopyrite | | | | | 0.11 | 0.00 | 0.07 | 0.00 | 0.22 | 0.00 | 0.25 | 0.00 |
| Sphalerite | | | 0.04 | 0.00 | | | | | | | | |
| Oxidized Fe-sulfide | 0.00 | 0.26 | 0.00 | 0.14 | 0.30 | 0.49 | 0.00 | 0.06 | 0.12 | 0.21 | 0.93 | 0.31 |
| Other | 0.59 | 1.40 | 0.21 | 1.86 | 0.37 | 1.43 | 1.58 | 1.40 | 0.83 | 0.70 | 0.87 | 0.93 |
| Total | 45.00 | 31.56 | 45.00 | 43.98 | 45.01 | 41.94 | 45.00 | 43.57 | 45.01 | 42.60 | 45.01 | 41.82 |

The masses of the samples decreased on average 9.1% in the HA2 extraction (Table 2). Especially, the amount of fine-grained particles appeared to decrease during the HA extraction (Figure 1 and Figures S1–S6) The highest decrease (29.9%) was observed for the sample WR1, which lost 13.4 g out of the original 45.0 g. The sample WR2 had the lowest mass decrease (2.3%); and of the original 45.0 g it lost 1.0 g.

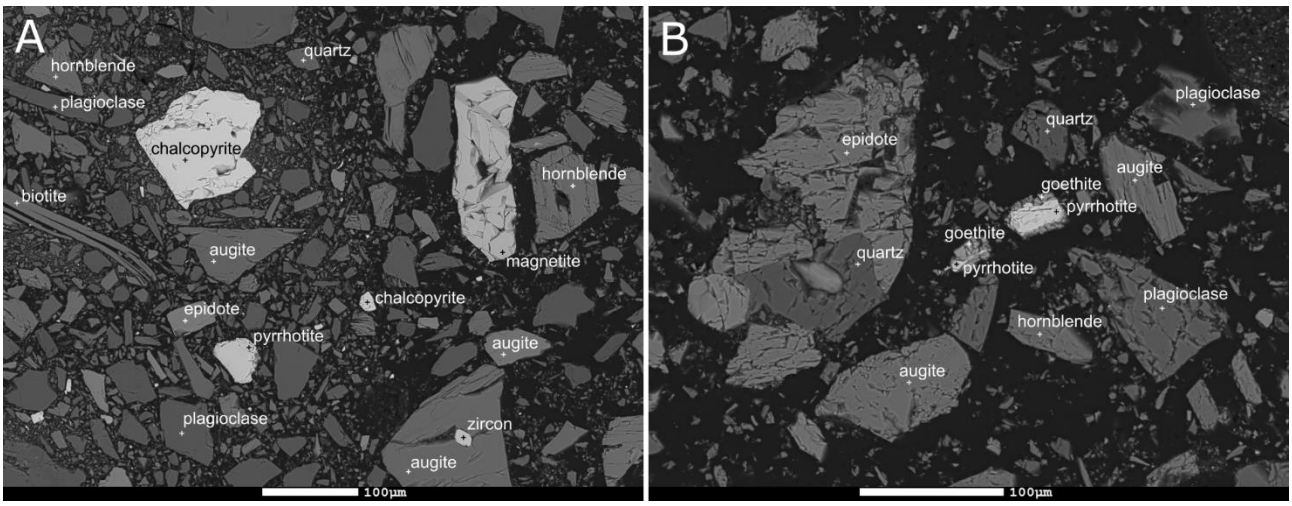


**Figure 1.** Backscattered electron images of the sample WR4 material before (**A**) and after (**B**) the HA2 extraction.

All detected sulfides were soluble in the HA2 (Table 2). Decomposition of pyrrhotite ($Fe_{1-x}S$) appeared to be incomplete in most samples. Backscattered electron images indicated that several pyrrhotite grains had a goethite (FeO(OH)) rim after the HA2 (e.g., Figure 1). Pyrite ($FeS_2$) did not completely decompose in the samples WR1 and WR2. According to backscattered electron images (Figure 2, Figures S1 and S2), some pyrite grains existed as inclusions inside quartz ($SiO_2$) in these samples. The other detected base metal sulfides pentlandite ($(Fe,Ni)_9S_8$), chalcopyrite ($CuFeS_2$) and sphalerite ((Zn,Fe)S) decomposed well in the HA2.

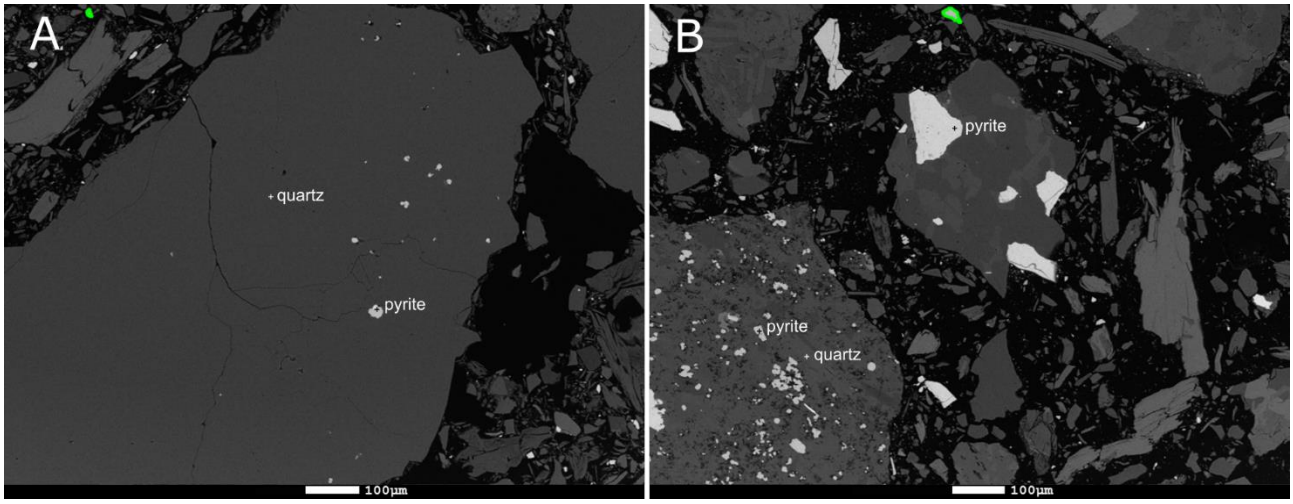


**Figure 2.** Backscatter electron images of the sample WR1 (**A**) and WR2 (**B**) showing pyrite inclusions in quartz.

Decomposition of different silicates in the HA2 extraction was variable (Table 2). Decomposition was detected for non-albite plagioclase ($(Na,Ca)(Si,Al)_4O_8$), albite ($NaAlSi_3O_8$), talc ($Mg_3Si_4O_{10}(OH)_2$), K-feldspar ($KAlSi_3O_8$), augite ($(Ca,Na)(Mg,Fe,Al,Ti)(Si,Al)_2O_6$), serpentine ($(Mg,Fe)_3Si_2O_5(OH)_4$), cordierite ($(Mg,Fe)_2Al_4Si_5O_{18}$) and kaolinite ($Al_2Si_2O_5(OH)_4$). For quartz, tremolite ($Ca_2Mg_5Si_8O_{22}(OH)_2$), phlogopite ($KMg_3AlSi_3O_{10}F(OH)$), muscovite ($(KAl_2(Si_3Al)O_{10}(OH, F)_2)$), hornblende ($(Ca,Na)_{2-3}(Mg,Fe,Al)_5(Al,Si)_8O_{22}(OH,F)_2$), olivine ($(Mg,Fe)_2SiO_4$), actinolite ($Ca_2(Mg,Fe)_5Si_8O_{22}(OH)_2$) and cummingtonite/enstatite ($(Mg,Fe^{2+})_2(Mg,Fe^{2+})_5Si_8O_{22}(OH)_2/MgSiO_3$) decomposition was detected in some samples, and quantitative increase in some samples. Quantitative increase was also detected for biotite ($K(Mg,Fe)_3(AlSi_3O_{10})(OH,F)_2$), diopside ($CaMgSi_2O_6$), chlorite ($(Mg,Fe)_5Al(Si_3Al)O_{10}(OH)_8$) and anthophyllite ($Mg_7(Si_8O_{22})(OH)_2$).

The detected carbonates magnesite ($MgCO_3$), dolomite ($CaMg(CO_3)_2$) and calcite ($CaCO_3$) were soluble in the HA2, but decomposed only partially (Table 2). In the WR4 sample the amount of calcite did not change in the HA2 extraction. In the WR1 sample, two thirds of the magnesite (4.61 g → 1.68 g) and most of the dolomite (1.33 g → 0.14 g) were decomposed. Calcite dissolution was the most efficient in the WR2 sample (0.96 g → 0.02 g), while in the WR4 sample the calcite content of 0.03 g did not change during the HA2 extraction.

### *3.2. Geochemical Results*

The parallel (HA1 and AR1) and sequential (HA2 and AR2) extraction results for Al, As, Ca, Cd, Co, Cr, Cu, Fe, K, Mg, Na, Ni, S and Zn, including total S, of the samples WR1-5b are presented in Table 3. The total S concentrations of the samples varied from 0.4% of WR4 to 5.3% of WR3. In general, the sulfide associated elements As (0.2–95 mg/kg), Co (13–166 mg/kg), Cu (92–4600 mg/kg), Ni (32–3210 mg/kg) and Zn (30–929 mg/kg) appeared as elevated concentrations, while Cd concentrations were relatively low (0.1–6.6 mg/kg).

**Table 3.** Total sulfur and the geochemical extraction results (mg/kg) of Al, As, Ca, Cd, Co, Cr, Cu, Fe, K, Mg, Na, Ni, S and Zn. AR = aqua regia, HA1 = $H_2O_2$-ammonium citrate extraction with normal sample amount, HA2 = $H_2O_2$-ammonium citrate extraction with large sample amount. Three parallel analysis were performed for HA1, these values are presented as averages of the three measurements ± standard deviation ($n$ = 3). AR2 (which was made for the residue of the HA2) results were adjusted for the original sample mass by a correlation factor (mass of residue / mass of original sample).

| Sample | Total S | Extraction Method | Al | As | Ca | Cd | Co | Cr | Cu | Fe | K | Mg | Na | Ni | S | Zn |
|---|---|---|---|---|---|---|---|---|---|---|---|---|---|---|---|---|
| WR1 | 22,500 | AR1 | 19,150 | 95 | 10,300 | 0.9 | 38 | 240 | 92 | 57,100 | 11,650 | 46,350 | 453 | 666 | 22,300 | 145 |
| | | HA1 | 256 ± 26 | 76 ± 9 | 3943 ± 21 | 0.6 ± 0.03 | 24 ± 0.7 | 6.5 ± 0.6 | 88 ± 0.5 | 2882 ± 946 | 319 ± 20 | 2262 ± 176 | 56 ± 28 | 525 ± 31 | 3722 ± 1520 | 68 ± 0.3 |
| | | HA2 | 281 | 68 | 3960 | 0.5 | 25 | 6.8 | 87 | 3160 | 320 | 2480 | 54 | 535 | 4140 | 68 |
| | | AR2 after HA2 | 14,164 | 29 | 2756 | 0.1 | 6.3 | 175 | 1.6 | 35,024 | 8414 | 30,431 | 327 | 65 | 6510 | 36 |
| WR2 | 41,800 | AR1 | 30,700 | 60 | 28,000 | 6.6 | 29 | 80 | 242 | 67,000 | 15,700 | 24,200 | 1580 | 359 | 41,200 | 929 |
| | | HA1 | 859 ± 67 | 28 ± 1.9 | 20,033 ± 473 | 2.7 ± 0.4 | 13 ± 0.2 | 2.6 ± 0.3 | 239 ± 10 | 15,033 ± 153 | 896 ± 67 | 979 ± 25 | 122 ± 21 | 252 ± 2 | 16,133 ± 1358 | 642 ± 9 |
| | | HA2 | 790 | 31 | 3940 | 1.9 | 13 | 1.8 | 243 | 14,700 | 842 | 1000 | 111 | 246 | 15,600 | 666 |
| | | AR2 after HA2 | 31,370 | 21 | 7984 | 0.4 | 8.9 | 112 | 2.4 | 38,015 | 15,929 | 27,168 | 1515 | 66 | 7173 | 90 |
| WR3 | 53,100 | AR1 | 20,900 | 1.7 | 1870 | 1.0 | 47 | 48 | 1680 | 96,000 | 11,000 | 18,200 | 469 | 2130 | 47,500 | 289 |
| | | HA1 | 619 ± 129 | 1.0 ± 0.2 | 460 ± 79 | 0.9 ± 0.1 | 39 ± 0.8 | 1.3 ± 0.1 | 1640 ± 53 | 8500 ± 348 | 693 ± 19 | 486 ± 53 | 127 ± 21 | 1823 ± 32 | 10,947 ± 1724 | 215 ± 6 |
| | | HA2 | 818 | 1.1 | 406 | 0.9 | 40 | 1.4 | 1670 | 10,000 | 699 | 579 | 101 | 1880 | 14,300 | 222 |
| | | AR2 after HA2 | 18,919 | 1.3 | 1417 | 0.3 | 6.8 | 44 | 580 | 68,779 | 9786 | 16,589 | 399 | 240 | 23,019 | 67 |

**Table 3.** *Cont.*

| Sample | Total S | Extraction Method | Al | As | Ca | Cd | Co | Cr | Cu | Fe | K | Mg | Na | Ni | S | Zn |
|---|---|---|---|---|---|---|---|---|---|---|---|---|---|---|---|---|
| WR4 | 3800 | AR1 | 13,200 | 0.6 | 15,100 | 0.2 | 13.3 | 20 | 2280 | 17,700 | 1120 | 3500 | 1900 | 32 | 3690 | 30 |
| | | HA1 | 249 ± 16 | 0.2 ± 0.04 | 1343 ± 90 | 0.1 ± 0.01 | 5.2 ± 0.3 | <1 | 1863 ± 32 | 2090 ± 26 | 61 ± 5 | 111 ± 10 | 133 ± 21 | 9.4 ± 0.6 | 1607 ± 93 | 16 ± 1.1 |
| | | HA2 | 271 | <0.2 | 1290 | 0.1 | 5.0 | <1 | 1920 | 2120 | <50 | 127 | 118 | 9.8 | 1560 | 14 |
| | | AR2 after HA2 | 12,876 | 0.5 | 13,651 | <0.04 | 7 | 21 | 89 | 14,425 | 1036 | 3301 | 1762 | 19 | 958 | 15 |
| WR5a | 15,400 | AR1 | 8440 | 0.2 | 3210 | 0.1 | 124 | 296 | 2920 | 61,200 | 1810 | 59,000 | 465 | 2170 | 13,900 | 43 |
| | | HA1 | 353 ± 35 | 0.2 ± 0.08 | 590 ± 81 | 0.1 ± 0.01 | 102 ± 1 | 8.3 ± 0.6 | 2747 ± 25 | 6120 ± 845 | 131 ± 5 | 3533 ± 448 | 151 ± 12 | 2007 ± 23 | 4647 ± 722 | 29 ± 1.2 |
| | | HA2 | 443 | <0.2 | 530 | 0.1 | 107 | 10.3 | 2840 | 7630 | 129 | 5160 | 140 | 2030 | 6120 | 28 |
| | | AR2 after HA2 | 8178 | <0.08 | 2934 | <0.04 | 22 | 310 | 133 | 50,547 | 1666 | 51,967 | 377 | 277 | 6039 | 19 |
| WR5b | 21,000 | AR1 | 4990 | 0.2 | 3040 | 0.2 | 166 | 501 | 4600 | 76,500 | 881 | 60,400 | 417 | 3210 | 21,100 | 59 |
| | | HA1 | 240 ± 15 | 0.2 ± 0.05 | 662 ± 104 | 0.2 ± 0.02 | 154 ± 3 | 13.4 ± 0.7 | 4643 ± 84 | 9050 ± 1518 | 38.4 ± 23 | 4510 ± 520 | 197 ± 5 | 3213 ± 25 | 7803 ± 1065 | 45 ± 2 |
| | | HA2 | 284 | <0.2 | 562 | 0.2 | 158 | 15.4 | 4620 | 11,000 | 50.5 | 6180 | 194 | 3200 | 9950 | 46 |
| | | AR2 after HA2 | 4860 | 0.1 | 2723 | <0.04 | 20 | 523 | 122 | 63,560 | 840 | 52,595 | 279 | 281 | 8902 | 17 |

The comparison of the HA1 and HA2 extraction results with the corresponding AR1 and AR2 extraction results is presented in Figure 3. As, Cd, Co, Cu, Ni, S and Zn were readily leachable in the HA extraction (Figure 3). The leaching of Cu was the highest, on average 94% (min 74% in WR3/HA2, max 100% in WR5b/HA1) compared with the AR extraction results. Average leaching of Cd was 79% (min 41% in WR2/HA1, max 100 in WR5a/HA1 and WR5b/HA1), of Ni 77% (min 29% in WR4/HA1, max 100% in WR5b/HA1), of Co 70% (min 39 in WR4/HA1, max 93% in WR5b/HA1), of Zn 67% (min 47% in WR1/HA1, max 88% in WR2/HA2), and of As 61% (min 17% in WR4/HA2, max 100% in WR5a/HA1 and WR5b/HA1).

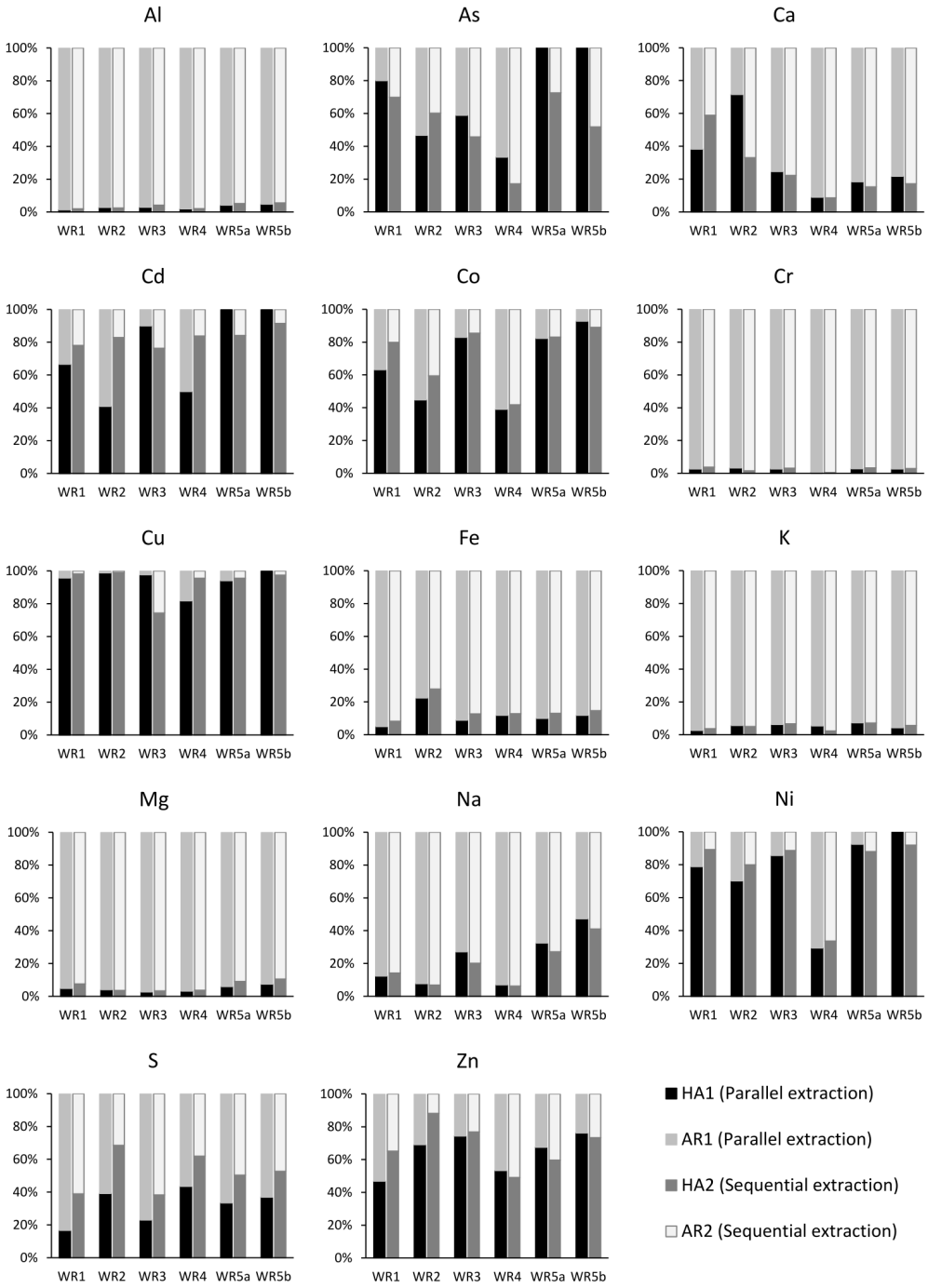


**Figure 3.** The HA1 and HA2 extraction results compared with the corresponding AR1 and AR2 extraction results of the samples WR1-5b. The AR extractable values as 100% (HA2 + AR2 for the sequential extraction).

The average S leachability in the HA extraction was 42% (min 17% in WR1/HA1, max 69% in WR2/HA2). Intense gas forming was observed for high-S samples (WR2 and WR3) during the HA extraction. When comparing the S leachabilities in the HA1 and HA2 extractions, it can be noted that the leaching of S in the HA2 was proportionally higher in comparison with the HA1 (Figure 3). Furthermore, the S concentrations in the AR1 were 1172–18427 mg/kg higher than the HA2 + AR2 S concentrations (Table 3).

Less elevated average leachabilities were measured for Ca, Na and Fe. Average leaching of Ca was 28% (min 9% in WR4/HA2, max 72% in WR2/HA1), of Na 21% (min 6% in WR4/HA2, max 47% in WR5a/HA1) and of Fe 13% (min 5% in WR1/HA1, max 28% in WR2/HA2).

Al, Cr, K and Mg were poorly leachable in the HA extraction. Average leaching of Al was 3% (min 1% in WR1/HA1, max 6% in WR5b/HA2), of Cr 3% (min 2% in WR2/HA2 and WR4/HA2, max 4% in WR1/HA1), of K 5% (min 2% in WR4/HA2, max 7% in WR3/HA2 and WR5a/HA1 and HA2) and of Mg 5% (min 3% in WR3/HA1 and HA2 and WR4/HA1, max 11% in WR5b/HA2).

The HA extraction results of the samples Mine A–Mine H, together with the AR extraction and drainage data obtained from Karlsson et al. [18], are presented in Table S2. The HA- and AR-extractable concentrations of Al, As, Cd, Co, Cr, Cu, Ni, S, Zn and the sums of As, Cd, Co, Cu, Ni and Zn in samples Mine A–Mine H and in the matching drainage waters are also presented in Figure 4 to show the correspondence of extractions with the observed drainage quality. It should be noted that in the cases of Mine A and Mine C new, the water samples were taken from a pond, not from seepage streams as the other water samples, which might be diluted by other water sources and, therefore, have lower overall drainage concentrations [18].

In general, the HA-extractable As, Cd, Co, Cr, Cu, Ni, S and Zn corresponded to the levels of drainage concentrations as shown in Figure 4. However, for Cd and Co the HA-extractable concentrations of the Mine C old and Mine C new samples did not correspond well with the drainage concentrations. In these cases, the HA extractable concentrations were notably greater than the concentrations in the drainage waters. Similarly, for Cu the HA-extractable concentrations of the Mine A sample did not correspond well with the relatively low drainage concentration. For Ni, the elevated HA-extractable concentration of the Mine C new sample did not correspond well with the relatively low drainage concentration. Either the lower HA-extractable Ni concentration did not reflect the elevated drainage concentration in the Mine B 2016 sample. For Zn, the HA-extractable concentration of the Mine A sample did not correspond well with the low drainage concentration, and the lower HA-extractable concentrations corresponded with the elevated drainage concentrations in samples Mine B 2016 and Mine H. The HA-extractable Al concentrations were in general low and did not correspond to the drainage concentrations of Mine A, Mine B 2016 and Mine H.

As presented in Karlsson et al. [18], in general the increase in the AR extractable As, Cd, Co, Cu, Ni and Zn concentrations followed that in the drainage concentrations. For Al, As, Cd, Co, Cu and Ni the elevated AR extractable concentrations did not correspond to elevated drainage concentrations in some circum-neutral water samples. Furthermore, the AR-extractable Cr concentrations were high in many cases and did not correlate with the low drainage concentrations.

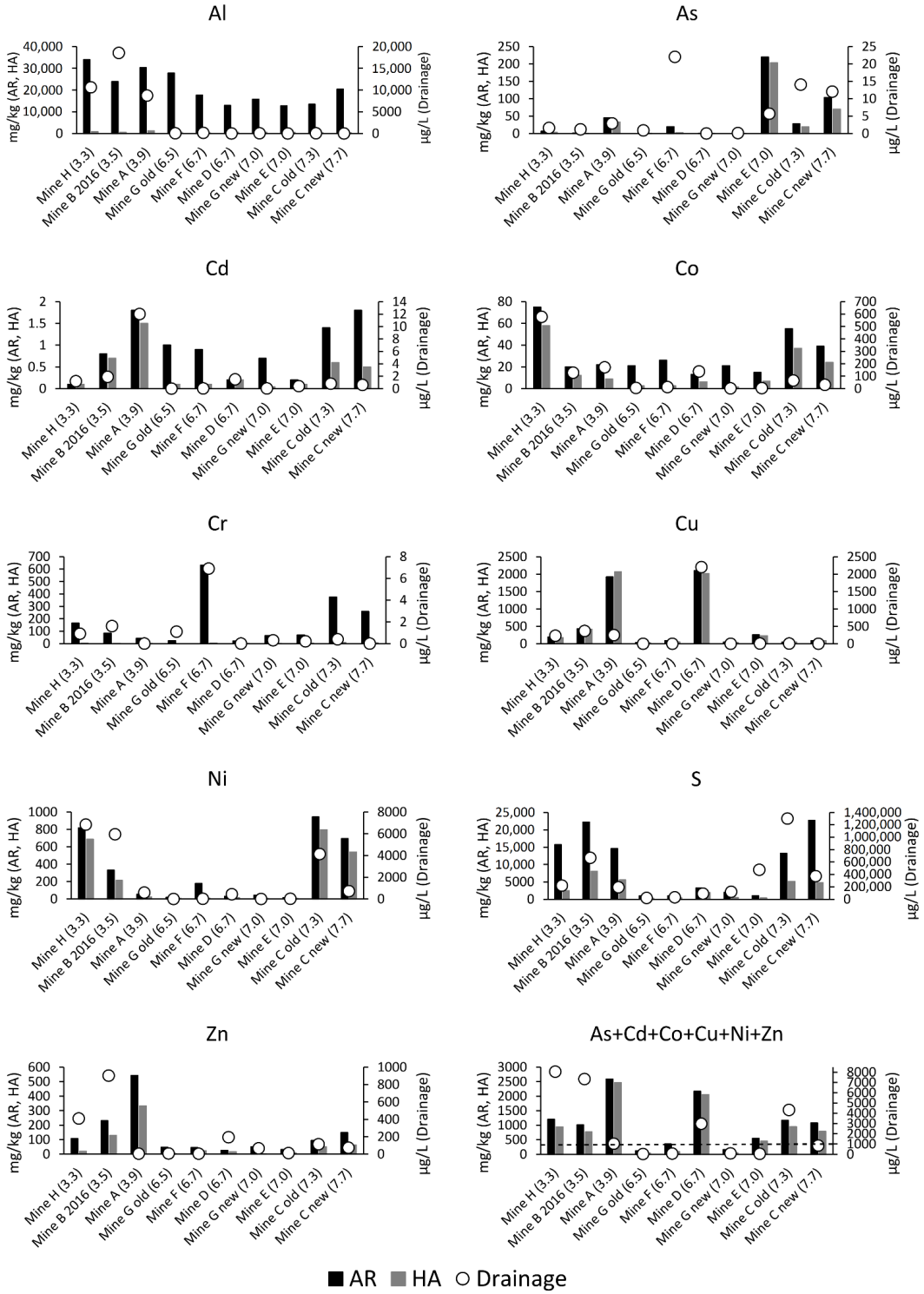


**Figure 4.** The HA and AR extractable concentrations of Al, As, Cd, Co, Cr, Cu, Ni, S, Zn and the sum of the As, Cd, Co, Cu, Ni and Zn concentrations in composite waste rock samples (histograms) and in the corresponding drainage water samples (dots). The drainage pH values are shown in brackets after the sample name. The samples are presented in the order of increasing drainage pH. Drainage and AR leach data are reported by Karlsson et al. [18]. The dashed black line presents 1000 µg/L in drainage for the sums of As, Cd, Co, Cu, Ni and Zn.

## 4. Discussion

### *4.1. Mineral Decomposition in the HA Extraction*

The mineralogical analyses showed that the Fe-sulfides pyrrhotite and pyrite did not completely dissolve in the HA extraction. Especially pyrrhotite dissolution rates were relatively low, ranging from total dissolution in the WR4 sample (0.05 g → 0 g) to apparent increase in WR5b (0.32 g → 0.41 g). Based on the results, the dissolution of pyrite was more efficient than that of pyrrhotite. In contrast, other base metal sulfides such as pentlandite, chalcopyrite and sphalerite were observed to dissolve efficiently.

Incomplete sulfide decomposition in the HA extraction has also been noticed in previous studies [24], as well as for other $H_2O_2$ based extraction methods, for example in the $H_2O_2$-ascorbic acid extraction [41], and in the single-addition NAG test [18,42–44]. Several reasons for this have been proposed. For example, the peroxide decomposition can be enhanced by metal ions released during sulfide oxidation [45]. Furthermore, the pyrrhotite micro-textures or mineral associations may control oxidation [46,47]. Furthermore, the precipitation of secondary minerals on sulfide surfaces may reduce the available surface area for oxidation [48].

Our results suggest that the incomplete dissolution of pyrite in the HA extraction could be partly caused by its occurrence in inclusions inside quartz, which can be observed in the backscattered electron images of the samples WR1 (Figure 2 and Figure S1) and WR2 (Figure 2 and Figure S2). Other sulfide species were not observed to occur in quartz inclusions. However, the precipitation of secondary minerals on pyrrhotite surfaces seems to play a major role in the incomplete pyrrhotite decomposition in the HA extraction. Several goethite rimmed pyrrhotite grains were observed in the backscattered electron images after the HA2 extraction (Figures S1, S2 and S4). Other sulfide species with secondary mineral coatings were not observed. Since larger amounts of sulfides were decomposed in the samples WR1–WR3 than in the sample WR5b which had only a few sulfides and minor pyrrhotite decomposition, the decomposition of peroxide seems to be less significant in the HA methods inefficiency e.g., than that of the NAG test.

The comparison of the HA results with the AR results showed that the chalcophile elements As, Cd, Co, Cu, Ni, S and Zn leached efficiently in the HA extraction in contrast to other elements (Al, Ca, Cr, Fe, K, Mg, Na). This supports the finding from the mineralogical results that the base metal sulfides oxidize and decompose effectively during the HA extraction. Especially the efficient leaching of Cu in HA compared with AR supports this finding since Cu occurs mainly in sulfides and rarely in silicates [49]. The fact that Cd, Co, Ni, Zn and As showed a high leaching rate in HA, but yet clearly smaller than that of Cu, is due to their occurrence in both sulfides and in other poorly soluble/weatherable minerals. For example, Cd, Co, Ni and Zn also occur in mafic silicates, e.g., olivine, pyroxenes, amphiboles and biotite [3,49], which are partially leachable in AR [11,13]. Furthermore, some Ni and Co can occur in pyrrhotite and pyrite [50,51], which decomposed incompletely in HA and, therefore, decreased their total extractability.

Based on our geochemical results, significant amounts of S appear to be lost during the HA extraction (Table 3). This can be observed by the fact that the initial S concentrations in the AR1 were clearly higher than the sum of S concentrations of the sequential HA2 and AR2 extractions. For example, in the cases of the samples WR1 and WR2, the HA2+AR2 S concentrations were only around half of the AR1 S concentrations. As the Fe-sulfide dissolution processes can produce $H_2S$ [52,53], it can be assumed that the S was lost due to gasification during the extraction.

The mineralogical results showed that the carbonate minerals identified as magnesite, dolomite and calcite, decomposed only incompletely in the HA extraction (Table 2). This finding is in accordance with the results by Parbhakar-Fox et al. [43] who reported incomplete decomposition of carbonates in the $H_2O_2$-based NAG test.

Both the mineralogical and geochemical results showed that decomposition of certain silicates occurred in the HA extraction, but the decomposition is clearly less complete than in the AR extraction. Furthermore, the extent of the decomposition in HA varies between

different silicates and different samples. Of the silicate minerals, the Ca and Mg bearing serpentine and non-albite plagioclase had notable (decrease of >4 g) decomposition in the HA2 extraction in some samples and minor decomposition in the rest of the samples (Tables 2 and 3). According to a minor decrease (>1 g) in mass and the HA solution analysis (especially Na concentration), albite and augite also appeared to experience slight decomposition in the HA extraction. Backscattered electron images showed that augite (see Figure S4), biotite (Figures S1 and S2), muscovite (Figure S3), plagioclase (Figures S3 and S4) and tremolite (Figure S1) were partially decomposed in the HA solution. Partial decomposition of silicates in the HA extraction has also been reported by Klock et al. [24]. However, according to the backscattered electron images the silicate decomposition is mainly etching of the mineral surfaces. This is supported by the fact that the silicate related element concentrations in the HA extraction are clearly lower in comparison with the AR extraction concentrations (Figure 3, Table 3).

Part of the decomposition of the silicates during the HA extraction was evidently additionally caused by the increase in the acidity of the solution due to sulfide oxidation. This is in accordance with the observations made in previous investigations, that the sulfuric acid produced by sulfide oxidation reactions during the $H_2O_2$-based extractions may lead to partial decomposition (i.e., etching) of silicates [22]. In addition, e.g., according to Dold [54], pyrite oxidation can produce high amounts of sulfuric acid. The silicate decomposition due to increased acidity as the results of sulfide oxidation was especially observed in the WR2 sample (total S 4.2%), where relatively high decomposition rates for albite, plagioclase and calcite were detected (Table 2). Furthermore, the amount of biotite in the high-S samples WR2 and WR3 appeared to increase relatively much, suggesting that acidic conditions might enhance biotite sheet separation. On the contrary, the WR4 sample with a relatively low amount of total S (0.4%) consisting of less acid liberating chalcopyrite and pyrrhotite [54], had no observable calcite decomposition.

Changes in the amounts of quartz in the HA2 extraction indicate that the interpretation of the mineralogical results is not unambiguous. It is expected that quartz does not decompose in HA. Nevertheless, the quantitative amounts of quartz had decreased in three samples (Table 2), notably much in the WR1 sample (20.94 g $\rightarrow$ 12.17 g). Furthermore, the quantitative amount of quartz had increased in two samples, especially in the WR2 sample (8.39 g $\rightarrow$ 13.16 g). This indicates that the mineralogical results before and after the HA2 extraction might involve some bias, which might be due to e.g., sorting of the sample material at some stage of the analyses. Furthermore, the decrease of fine-grained particles during the HA extraction, either by decomposition or sorting bias, might affect the relative proportions of some minerals. Furthermore, when considering the mineralogical results of this study, it must be noted that the SEM analysis after the HA2 was not done for exactly the same sample material as the SEM analysis before the HA2; the samples were parallel sub-samples of the larger powdered waste rock samples. Although the powdered samples are supposed to be relatively homogenous, some small variation might exist. To verify the mineralogical results, further investigations including several repetitions of the larger-scale HA2 extractions should be conducted.

### *4.2. HA Extraction in the Preliminary Element Mobility Assessment*

The comparison of the HA and the AR extraction results with the drainage quality data shows that the HA extraction data can be useful to preliminary assess the element mobility from the waste rock material. In the previous study by Karlsson et al. [18] it was shown that data from the waste rock AR extraction reflect element contents that occur in waste rock pile drainage water though it over-predicts Al, As, Cd, Co, Cu and Ni concentrations in some circum-neutral drainages, and Cr concentrations in general (Figure 4). Furthermore, if the AR-extractable sum of As, Cd, Co, Cu, Ni and Zn is >1000 mg/kg, it may indicate an elevated risk for high-metal (>1000 µg/L) drainage [18] (Figure 4).

Similar to the AR extraction, the concentrations of chalcophile elements As, Cd, Co, Cu, Ni, S and Zn analyzed in the HA extraction solution appear to predict elevated drainage

concentrations (Figure 4). In contrast to AR, the HA extractable Cr concentrations were low, corresponding well to the low drainage concentrations. For Al, the HA extractable concentrations were generally low, and they cannot be used to predict possibly elevated Al concentrations in acidic drainage systems. In general, the HA extractable element concentrations were below the corresponding AR concentrations. Based on the results, it can be generalized (Figure 4) that if the HA extractable sum of As, Cd, Co, Cu, Ni and Zn is >750 mg/kg, there is a high risk for high-metal drainage (the sum of harmful metals and metalloids >1000 µg/L, as in Plumlee et al. [55]). As discussed above in Section 4.1, HA is a more sulfide specific extraction method compared with the more aggressive AR extraction. The fact that HA dissolves less silicate bound elements, indicates that it might be more accurate in drainage quality assessment compared with the AR method.

In addition, the HA extraction seems to perform well in the assessment of element mobilities, if compared with the single-addition NAG test leachate analysis. Karlsson et al. [18] investigated the performance of the $H_2O_2$-based single-addition NAG test leachate analysis in the drainage quality prediction. Based on their results, the NAG test method was also useful for assessing the mobility of Al, Cd, Co, Cr, Cu, Ni and Zn. However, in some high-metal NRD cases the prediction underestimated the drainage concentrations due to the precipitation of most of the contaminants during the test when the NAG test leachate pH was above 3–6 [18]. According to our results, the performance of the HA method is similar, excluding Al, but the HA extraction performs well also for NRD cases.

Other extraction methods have also been shown to be sulfide specific, e.g., brominated water extraction, bromine-methanol extraction, brominated water-carbon tetrachloride and hydrogen peroxide-ascorbic acid extraction [24], but these methods have downsides when compared with the HA extraction. For example, due to the risks related to work safety, the handling of bromine-based solutions in laboratory demands additional caution [56]. Some methods are more time consuming, e.g., hydrogen peroxide-ascorbic acid extraction requires heating on a steam bath for 18 h [24].

Commonly-used methods to assess the element mobility from mine waste include sequential and parallel extraction procedures [57]. These methods are based on partitioning the solid sample material into specific fractions by a sequential or parallel series of selective extractions, with an aim to simulate the release of elements in various environmental conditions. For example, a sequential extraction method for Cu-sulfide mine wastes has been developed by Dold [10], and a parallel selective extraction method for Ni and Cu mine tailings by Heikkinen and Räisänen [3,58]. These procedures include the use of, among others, $NH_4$-oxalate extraction for e.g., Fe precipitates, $NH_4$-acetate extraction for e.g., exchangeable element fraction, and $H_2O$ extraction for water soluble fraction, together with stronger extractions for sulfide bound elements (e.g., AR) and silicate bound elements (e.g., $HNO_3$-HF-$HClO_4$-HCl digestion) [10]. However, the sequential and parallel methods are usually applied to investigate the already existing and weathered mine wastes, as especially the results of the weaker extractions reveal how the elements are currently bound, not how e.g., a fresh rock material will behave in future.

Based on the results, the HA and AR leachable concentrations do not unambiguously measure the actual concentrations of contaminants in drainage water, but merely predict their potential mobility caused by the sulfide oxidation and acid generation. The small-scale laboratory tests such as the HA and AR extractions are useful for preliminary screening in the drainage water quality assessment of waste rocks, but more thorough investigations, e.g., including kinetic testing and geochemical modeling, among others, should still be carried out to evaluate the drainage quality and the long-term behavior of extractive waste.

According to the previous studies, waste rock characterization and drainage quality predictions utilizing data from small-scale laboratory tests have limitations related e.g., to small sample size, crushing of the samples, mineral assemblage and surface area, rock texture and mineral impurities that might affect the weathering rate [54,59–62]. Furthermore, sampling is also one key issue in the test. The waste rock samples used in this study were composite samples collected from the surface of waste rock piles, which should be

considered when interpreting the results. In addition, drainage water samples represented only one sampling event. A longer lasting monitoring campaign is recommended, as the contaminant concentrations in mine waste drainage may display wide annual and seasonal fluctuations [63–66]. Our results related to element mobility assessment should be verified by a more thorough and longer lasting investigation.

## 5. Conclusions

The HA extraction provides a viable method for the characterization of extractive waste, being a more sulfide-specific method than the AR extraction. Sulfide minerals, especially base metal sulfides pentlandite, chalcopyrite and sphalerite, decomposed efficiently in the HA extraction. Fe-sulfides pyrrhotite and pyrite decomposed only incompletely. Especially the pyrrhotite dissolution rates were relatively low, which might be due to the precipitation of goethite on pyrrhotite surfaces.

The HA extraction also partially leached silicates and carbonates, but in general the AR extraction decomposes many minerals more efficiently. Especially, the Ca and Mg bearing minerals serpentine and non-albite plagioclase appear to be relatively decomposable in HA. Furthermore, only some minor decomposition of albite, augite, biotite, muscovite and tremolite was detected. The carbonate minerals calcite, dolomite and magnesite decomposed also incompletely in the HA extraction. The decomposition of silicates and carbonates is related to both the use of $H_2O_2$ in leaching and the amount of acid producing sulfides in the sample. The sulfuric acid produced by sulfide oxidation during the extraction enhances the partial decomposition of silicates and carbonates. This should be noted especially for the samples with high amounts of sulfides.

The study showed that the HA extraction results are useful in the preliminary assessment of the element mobilities. Based on the results, if the HA-extractable sum of As, Cd, Co, Cu, Ni and Zn is >750 mg/kg, there is an increased risk for high-metal (>1000 µg/L) drainage. In general, the elevated As, Cd, Co, Cu, Ni, S and Zn leachability in the HA extraction appears to predict elevated drainage concentrations. For Cr, the HA extraction predicted more realistic drainage concentrations compared with the AR extraction, which results in too high a Cr concentration. The HA extractable concentrations of Al were low and, therefore, they do not reveal the potential Al contamination in acidic drainage systems.

**Supplementary Materials:** The following are available online at https://www.mdpi.com/article/10.3390/min11070706/s1: Figure S1. Backscattered electron images before (upper) and after (lower) the $H_2O_2$ ammonium citrate extraction (HA2) of the sample WR1. Figure S2. Backscattered electron images before (upper) and after (lower) the $H_2O_2$ ammonium citrate extraction (HA2) of the sample WR2. Figure S3. Backscattered electron images before (upper) and after (lower) the $H_2O_2$ ammonium citrate extraction (HA2) of the sample WR3. Figure S4. Backscattered electron images before (upper) and after (lower) the $H_2O_2$ ammonium citrate extraction (HA2) of the sample WR4. Figure S5. Backscattered electron images before (upper) and after (lower) the $H_2O_2$ ammonium citrate extraction (HA2) of the sample WR5a. Figure S6. Backscattered electron images before (upper) and after (lower) the $H_2O_2$ ammonium citrate extraction (HA2) of the sample WR5b. Table S1. Mineralogy of the samples before and after the HA2 extraction based on FE-SEM-EDS. The identification of the main mineral phases verified by XRD. Mineral masses calculated by wt. % and the total mass of the sample. Table S2. Waste rock aqua regia (AR) and $H_2O_2$ ammonium citrate extraction (HA) results (mg/kg), and corresponding waste rock pile drainage data (µg/L) from several Finnish mine sites. Mine site descriptions, and drainage and AR data from Karlsson et al. [18].

**Author Contributions:** Conceptualization, T.K. and M.L.R.; methodology, T.K., T.M., M.L. and M.L.R.; resources, P.K.; writing—original draft preparation, T.K.; writing—review and editing, T.K., M.L.R., T.M., L.A., M.L. and P.K.; visualization, T.K.; supervision, L.A. and P.K.; funding acquisition, T.K. and P.K. All authors have read and agreed to the published version of the manuscript.

**Funding:** The writing of this article was funded by K.H. Renlund's Foundation. The samples for this study were obtained as part of GTK's projects: Closedure project (2012–2015), funded by the TEKES Green Mining Programme (project code 40364/12), and the KaiHaMe project (2015–2018), funded by

the European Regional Development Fund (project code A70565). The analyses were conducted with GTK's internal funding.

**Data Availability Statement:** Data for this study are presented in the paper and cited references.

**Conflicts of Interest:** The authors declare no conflict of interest.

## References


1. Robb, L. *Introduction to Ore-Forming Processes*; Blackwell Publishing: Oxford, UK, 2004.
2. Dold, B. Evolution of acid mine drainage formation in sulfidic mine tailings. *Minerals* **2014**, *4*, 621–641. [CrossRef]
3. Heikkinen, P.M.; Räisänen, M.L. Trace metal and as solid-phase speciation in sulfide mine tailings–indicators of spatial distribution of sulfide oxidation in active tailings impoundments. *Appl. Geochem.* **2009**, *24*, 1224–1237. [CrossRef]
4. Acid Rock Drainage Prediction Manual. Available online: http://mend-nedem.org/wp-content/uploads/2013/01/1.16.1b.pdf (accessed on 14 October 2020).
5. Price, W.A. Challenges posed by metal leaching and acid rock drainage, and approaches used to address them. In *Environmental Aspects of Mine Wastes, Short Course Series*; Jambor, J.L., Blowes, D.W., Ritchie, A.I.M., Eds.; Mineralogical Association of Canada: Quebec, QC, Canada, 2003; Volume 31, pp. 15–30.
6. Singer, P.C.; Stumm, W. Acid mine drainage: The rate-determining step. *Science* **1970**, *167*, 1121–1123. [CrossRef]
7. Blowes, D.W.; Ptacek, C.J. Acid-neutralization mechanisms in inactive mine tailings. In *The Environmental Geochemistry of Sulfide Mine Wastes, Short Course Series*; Jambor, J.L., Blowes, D.W., Eds.; Mineralogical Association of Canada: Quebec, QC, Canada, 1994; Volume 31, pp. 95–116.
8. Fletcher, W.K. (Ed.) *Handbook of Exploration Geochemistry—Volume 1: Analytical Methods in Geochemical Prospecting*; Elsevier Scientific Publishing Company: Amsterdam, The Netherlands, 1981.
9. Lynch, J.J. The determination of copper, nickel and cobalt in rocks by atomic absorption spectrometry using a cold leach. *J. Geochem. Explor.* **1971**, *11*, 313–315.
10. Dold, B. Speciation of the most soluble phases in a sequential extraction procedure adapted for geochemical studies of copper sulfide mine waste. *J. Geochem. Explor.* **2003**, *80*, 55–68. [CrossRef]
11. Niskavaara, H. A comprehensive scheme of analysis for soils, sediments, humus and plant samples using inductively coupled plasma atomic emission spectrometry (ICP-AES). In *Geological Survey of Finland, Current Research 1993–1994*; Special Paper 20; Autio, S., Ed.; Geological Survey of Finland: Espoo, Finland, 1995; pp. 167–175.
12. Muniruzzaman, M.; Kauppila, P.M.; Karlsson, T. *Water Quality Prediction of Mining Waste Facilities Based on Predictive Models*; Geological Survey of Finland: Espoo, Finland, 2018.
13. Doležal, J.; Provondra, P.; Šulcek, Z. *Decomposition Techniques in Inorganic Analysis*; Iliffe Books Ltd.: London, UK, 1968.
14. Finnish Government. *Government Decree on Extractive Waste 190/2013*; Finnish Government: Helsinki, Finland, 2013. Available online: https://www.finlex.fi/fi/laki/kaannokset/2013/en20130190_20150102.pdf (accessed on 14 October 2020).
15. Fosso-Kankeu, E.; Waanders, F.; Mulaba-Bafubiandi, A.; Sidu, S. Leachability of suspended particles in mine water and risk of water contamination. In Proceedings of the 10th ICARD and IMWA 2015 Conference, Santiago, Chile, 21–24 April 2015; Brown, A., Bucknam, C., Burgess, J., Carballo, M., Castendyk, D., Figueroa, L., Eds.; Gecamin Publications: Santiago, Chile, 2015; pp. 788–796.
16. Karlsson, T.; Kauppila, P.M. Waste rock characterization versus the actual seepage water quality. In Proceedings of the International Mine Water Association 2016 Symposium Mining Meets Water—Conflicts and Solutions, Leipzig, Germany, 11–15 July 2016; Drebenstedt, C., Paul, M., Eds.; TU Bergakademie: Freiberg, Germany, 2016; pp. 402–406.
17. Karlsson, T.; Kauppila, P.M.; Lehtonen, M. Prediction of the long-term behaviour of extractive wastes based on environmental characterisation: Correspondence of laboratory prediction tests with field data. *Bull. Geol. Surv. Finl.* **2018**, *408*, 11–26.
18. Karlsson, T.; Alakangas, L.; Kauppila, P.M.; Räisänen, M.L. A test of two methods for waste rock drainage quality prediction: Aqua regia extraction and single-addition net-acid generation test leachate analysis. *Mine Water Environ.* **2021**. [CrossRef]
19. Price, W.A.; Morin, K.; Hutt, N. Guidelines for prediction of acid rock drainage and metal leaching for mines in British Columbia: Part II. In Proceedings of the Recommended procedures for static and kinetic tests. In Proceedings of the 4th ICARD Conference, Vancouver, BC, Canada, 1 June 1997; Gusek, J., Wildeman, T., Eds.; Volume 1, pp. 15–30.
20. Katsnelson, E.M.; Osipova, J.J. Usoveršenstvovannyi metod opredelenija sul'fidnogo nikelja. *Obogaštšenie* **1960**, *4*, 24–26, (with English abstract).
21. Czamanske, G.K.; Ingamells, C.O. Selective chemical dissolution of sulfide minerals: A method of mineral separation. *Am. Mineral.* **1970**, *55*, 2131–2134.
22. Penttinen, U.; Palosaari, V.; Siura, T. Selective dissolution and determination of sulfides in nickel ores by the bromine-methanol method. *Bull. Geol. Soc. Finl.* **1977**, *49*, 79–84. [CrossRef]
23. Karapetyan, E.T. Opredelenie sul'fidnogo nikelya v sul'fidnykh rudakh I kontsentratakh. *Zavod. Lab.* **1968**, *34*, 939–940, (with English abstract).
24. Klock, P.R.; Czamanske, G.K.; Foose, M.; Pesek, J. Selective chemical dissolution of sulfides: An evaluation of six methods applicable to assaying sulfide-bound nickel. *Chem. Geol.* **1986**, *54*, 157–163. [CrossRef]
25. Bradley, J.; Baker, H. *Mineral Resource Estimate for the Rönnbäcken Nickel Project, Sweden*; SRK Consulting: Skellefteå, Sweden, 2010.

26. Gray, D.; Cameron, T.; Briggs, A. *Kevitsa Nickel Copper Mine, Lapland, Finland*; NI 43-101 Technical Report; First Quantum Minerals: West Perth, Australia, 2016.
27. Peters, L.J. *Beaver and Lynx Sulfide Nickel Property (BL Property), Cariboo Mining Division, British Columbia*; National Instrument 43-101 Technical Report; Inomin Mines Inc.: Vancouver, BC, Canada, 2020.
28. Kuronen, E.; Tuokko, I. Horsmanaho Talc Mine. In *Excursion Guidebook A4—Ore Deposits in Eastern Finland, Proceedings of the 4th Biennial SGA Meeting, Turku, Finland, 11–13 August 1997*; Loukola-Ruskeeniemi, K., Sorjonen-Ward, P., Eds.; Geological Survey of Finland: Espoo, Finland, 1997; Guide 42; pp. 39–42.
29. Kontinen, A.; Peltonen, P.; Huhma, H. *Description and Genetic Modelling of the Outokumpu-Type Rock Assemblage and Associated Sulfide Deposits*; Geological Survey of Finland: Espoo, Finland, 2006; Archive Report M 10.4/2006/1.
30. Meriläinen, M.; Ekberg, M.; Lovén, P.; Koivistoinen, P.; Hakola, J.; Strauss, T. *Updated Reserve and Resource Estimate of the Hitura Nickel Mine in Central Finland*; National Instrument 43–101, Technical Report; Belvedere Resources: Preston, UK, 2008.
31. Makkonen, H. Hitura Ni. In *Metallogenic Areas in Finland*; Special Paper 53; Geological Survey of Finland: Espoo, Finland, 2012; pp. 207–342.
32. Hyvärinen, L. On the geology of the copper ore field in the Virtasalmi area, Eastern Finland. *Bull. Comm. Géologique Finl.* **1969**, *240*, 82.
33. Lawrie, K.C. Geochemical characterisation of a polyphase deformed, altered and high grade metamorphosed volcanic terrane: Implications for the tectonic setting of the Svecofennides, South-Central Finland. *Precambrian Res.* **1987**, *59*, 171–205. [CrossRef]
34. Papunen, H. Suomen metalliset malmiesiintymät. In *Suomen Malmigeologia—Metalliset Malmiesiintymät*; Papunen, H., Haapala, I., Rouhunkoski, P., Eds.; Suomen Geologinen Seura ry: Mänttä, Finland, 1986. (In Finnish)
35. Geological Survey of Finland. *Mineral Deposit Report 103: Virtasalmi*; Geological Survey of Finland, Mineral Deposits-Report Database; Available online: http://tupa.gtk.fi/karttasovellus/mdae/raportti/103_Virtasalmi.pdf (accessed on 22 January 2018).
36. Santaguida, F.; Luolavirta, K.; Lappalainen, M.; Ylinen, J.; Voipio, T.; Jones, S. The Kevitsa Ni-cu-PGE deposit in the Central Lapland greenstone belt in Finland. In *Mineral Deposits of Finland*; Maier, W., Lahtinen, R., O'Brien, H., Eds.; Elsevier: Amsterdam, The Netherlands, 2015; pp. 195–210.
37. ISO/IEC. *General Requirements for the Competence of Testing and Calibration Laboratories*; International Organization for Standardization: Geneva, Switzerland, 2005; DIN ISO/IEC 17025:2005-11.
38. ISO. *Soil Quality—Determination of Total Sulfur by Dry Combustion*; International Organization for Standardization: Geneva, Switzerland, 2000; DIN ISO 115178:2000-11.
39. ISO. *Soil Quality—Extraction of Trace Elements Soluble in Aqua Regia*; International Organization for Standardization: Geneva, Switzerland, 1995; DIN ISO 11466:1995-03.
40. Young, R.S. *Chemical Phase Analysis*; Charles Griffin and Company Ltd.: London, UK, 1974; p. 138.
41. Chao, T.T.; Sanzolone, R.J. Chemical dissolution of sulfide minerals. *J. Res. US Geol. Surv.* **1977**, *5*, 409–412.
42. Karlsson, T.; Räisänen, M.L.; Lehtonen, M.; Alakangas, L. Comparison of static and mineralogical ARD prediction methods in the Nordic environment. *Environ. Monit. Assess* **2018**, *190*, 719. [CrossRef]
43. Parbhakar-Fox, A.; Fox, N.; Ferguson, T.; Hill, R.; Maynard, N. Dissection of the NAG pH test: Tracking efficacy through examining reaction products. In Proceedings of the 11th ICARD—IMWA—MWD Conference, Pretoria, South Africa, 10–14 September 2018; Wolkersdorfer, C., Sartz, L., Weber, A., Burgess, J., Tremblay, G., Eds.; International Mine Water Association: Wendelstein, Germany, 2018; pp. 949–955.
44. Stewart, W.A. Development of Acid Rock Drainage Prediction Methodologies for Coal Mine Wastes. Ph.D. Thesis, University of South Australia, Adelaide, Australia, 2005.
45. AMIRA. Prediction and kinetic control of acid mine drainage. In *ARD Test Handbook*; Project P387A; AMIRA International: Melbourne, Australia, 2002.
46. Kwong, Y.T.J. *Prediction and Prevention of Acid Rock Drainage from a Geological and Mineralogical Perspective*; MEND Report 1.32.1; Ottawa, ON, Canada; Available online: http://mend-nedem.org/wp-content/uploads/1.32.1.pdf (accessed on 14 October 2020).
47. Parbhakar-Fox, A.; Lottermoser, B.; Bradshaw, D. Evaluating waste rock mineralogy and microtexture during kinetic testing for improved acid rock drainage prediction. *Miner. Eng.* **2013**, *52*, 111–124. [CrossRef]
48. Al, T.A.; Blowes, D.W.; Martin, C.J.; Cabri, L.J.; Jambor, J.L. Aqueous geochemistry and analysis of pyrite surfaces in sulfide-rich mine tailings. *Geochim. Cosmochim. Acta* **1997**, *61*, 2353–2366. [CrossRef]
49. Koljonen, T. *The Geochemical Atlas of Finland. Part 2: Till*; Geological Survey of Finland: Espoo, Finland, 1992.
50. Campbell, F.A.; Ethier, V.G. Nickel and cobalt in pyrrhotite and pyrite from the Faro and Sullivan orebodies. *Canad. Mineral.* **1984**, *22*, 503–506.
51. Liu, Z.; Shao, Y.; Zhou, H.; Liu, N.; Huang, K.; Liu, Q.; Zhang, J.; Wang, C. Major and Trace element geochemistry of pyrite and pyrrhotite from stratiform and lamellar orebodies: Implications for the ore genesis of the dongguashan copper (gold) deposit, Eastern China. *Minerals* **2018**, *8*, 380. [CrossRef]
52. Belzile, N.; Chen, Y.W.; Cai, M.F.; Li, Y. A review on pyrrhotite oxidation. *J. Geochem. Explor.* **2004**, *84*, 65–76. [CrossRef]
53. Ding, K.; Liu, Y. Hydrolysis of Pyrite: A Possible pathway for generation of high concentrations of $H_2S$ gas in deep-buried reservoirs? *Dev. Earth Sci.* **2017**, *5*, 1–8. [CrossRef]
54. Dold, B. Acid rock drainage prediction: A critical review. *J. Geochem. Explor.* **2017**, *172*, 120–132. [CrossRef]

55. Plumlee, G.S.; Smith, K.S.; Mountour, M.R.; Ficklin, W.H.; Mosier, E.L. Geologic controls on the composition of natural waters and mine waters draining diverse mineral-deposit types. *Rev. Econ. Geol.* **1999**, *6*, 373–432.
56. *Bromine Safety Handbook*; India Bromine Platform: Mumbai, India, 18 March 2019; pp. 36–65. Available online: https://www.indianchemicalcouncil.com/docs/Bromine-Safety-Handbook.pdf (accessed on 16 June 2021).
57. Kauppila, P.M. Sequential Extraction Procedure. Available online: https://mineclosure.gtk.fi/sequential-extraction-procedure/ (accessed on 16 June 2021).
58. Heikkinen, P.M.; Räisänen, M.L. Mineralogical and geochemical alteration of Hitura sulphide mine tailings with emphasis on nickel mobility and retention. *J. Geochem. Explor.* **2008**, *97*, 1–20. [CrossRef]
59. Jambor, J.L. Mine-waste mineralogy and mineralogical perspectives of acid-base accounting. In *The Environmental Geochemistry of Sulfide Mine-Wastes, Short Course Handbook*; Jambor, J.L., Blowes, D.W., Eds.; Mineralogical Association of Canada: Ottawa, ON, Canada, 2002; Volume 22, pp. 59–102.
60. Paktunc, A.D. Mineralogical constrains of the determination of neutralization potential and prediction of acid mine drainage. *Environ. Geol.* **1999**, *39*, 103–112. [CrossRef]
61. Parbhakar-Fox, A.; Lottermoser, B.G. A critical review of acid rock drainage prediction methods and practices. *Miner. Eng.* **2015**, *82*, 107–124. [CrossRef]
62. White, W.W., III; Lapakko, K.A.; Cox, R.L. Static-test methods most commonly used to predict acid mine drainage: Practical guidelines for use and interpretation. In *The Environmental Geochemistry of Mineral Deposits, Part A: Processes, Techniques, and Health Issues*; Reviews in Economic Geology; Plumlee, G.S., Logsdon, M.J., Filipek, L.F., Eds.; Society of Economic Geologists: Littleton, CO, USA, 1999; pp. 325–328.
63. Alakangas, L.; Lundberg, A.; Öhlander, B. Estimation of temporal changes in oxidation rates of sulfides in copper mine tailings at Laver, Northern Sweden. *Sci. Total Environ.* **2010**, *408*, 1386–1392. [CrossRef]
64. González, R.M.; Cánovas, C.R.; Olías, M.; Macías, F. Seasonal variability of extremely metal rich acid mine drainages from the Tharsis mines (SW Spain). *Environ. Pollut.* **2020**, *259*, 113829. [CrossRef] [PubMed]
65. Heikkinen, P.M.; Räisänen, M.L.; Johnson, R.H. Geochemical characterisation of seepage and drainage water quality from two sulfide mine tailings impoundments: Acid mine drainage versus neutral mine drainage. *Mine Water Environ.* **2009**, *28*, 30–49. [CrossRef]
66. Søndergaard, J.; Elberling, B.; Asmund, G.; Gudrum, C.; Iversen, K.M. Temporal trends of dissolved weathering products from a high Arctic coal mine waste rock pile in Svalbard (78° N). *Appl. Geochem.* **2007**, *22*, 125–138. [CrossRef]